Arabian Journal of Chemistry (2018) **11**, 291–304

King Saud University

Arabian Journal of Chemistry

www.ksu.edu.sa
www.sciencedirect.com

ORIGINAL ARTICLE

Highly water-soluble ruthenium(II) terpyridine coordination compounds form stable adducts with blood-borne metal transporting proteins

Marija Nišavić [a], Milovan Stoiljković [a], Ivo Crnolatac [b], Maja Milošević [c], Ana Rilak [d], Romana Masnikosa [a,*]

[a] *Department of Physical Chemistry, Vinča Institute of Nuclear Sciences, University of Belgrade, Mike Petrovića Alasa 12-14, 11000 Belgrade, Serbia*
[b] *Division of Organic Chemistry and Biochemistry, Ruđer Bošković Institute, Bijenička cesta 54, 10000 Zagreb, Croatia*
[c] *Department of Molecular Biology and Endocrinology, Vinča Institute of Nuclear Sciences, University of Belgrade, Mike Petrovića Alasa 12-14, 11000 Belgrade, Serbia*
[d] *Department of Chemistry, Faculty of Science, University of Kragujevac, Radoja Domanovića 12, 34000 Kragujevac, Serbia*

Received 14 May 2016; revised 26 July 2016; accepted 27 July 2016
Available online 4 August 2016

KEYWORDS

Anticancer drugs;
Ru(II) terpyridine coordination compounds;
Serum albumin binding;
Serum transferrin binding;
CD spectra;
ESI qTOF MS spectra

Abstract Three coordination compounds of ruthenium(II), belonging to a recently synthesised series of water-soluble compounds of general formula *mer*-[Ru(L_3)(N-N)Cl]Cl, where L_3 = 4'-chloro-2,2':6',2″-terpyridine (Cl-tpy), N-N = ethylenediamine (en), 1,2-diaminocyclohexane (dach) or 2,2'-bipyridine (bpy), have shown strong binding to calf thymus DNA and moderate *in vitro* cytotoxicity towards cancer cell lines. Knowing that serum proteins play a crucial role in the transport and deactivation of ruthenium drugs, we have conducted a detailed study of their interactions with two major metal-transporting serum proteins, albumin and transferrin, and it is presented herein. Ruthenated protein adducts were formed with various concentrations of the three compounds and then separated from the unbound portions by ultrafiltration through 10 kDa cut-off centrifugal filter units. The stoichiometry of binding was determined using inductively coupled plasma optical emission spectrometry. One mol of albumin bound up to 7, 8.5 and 1.5 mol of compound **1** ([Ru(Cl-tpy)(en)Cl][Cl]), **2** ([Ru(Cl-tpy)(dach)Cl][Cl] and **3** ([Ru(Cl-tpy)(bpy)Cl][Cl]), respectively. One mol of transferrin bound up to 3, 3.5 and 0.4 mol of **1**, **2** and **3**, respectively. The affinity of albumin and

* Corresponding author. Fax: +381 11 2408 635.
E-mail addresses: marija.nisavic@vin.bg.ac.rs (M. Nišavić), missa@vin.bg.ac.rs (M. Stoiljković), Ivo.Crnolatac@irb.hr (I. Crnolatac), mmilosevic@vin.bg.ac.rs (M. Milošević), anarilak@kg.ac.rs (A. Rilak), masnikosa_romana@yahoo.co.uk, romana@vin.bg.ac.rs (R. Masnikosa).
Peer review under responsibility of King Saud University.

Production and hosting by Elsevier

http://dx.doi.org/10.1016/j.arabjc.2016.07.021

transferrin for the three ruthenium compounds was evaluated using fluorescence quenching. The binding constants for **1** and **2** lay within the range 10^4–10^5 M^{-1}, suggesting moderate-to-strong attachment to albumin. Both compounds showed much lower affinity for transferrin (10^2–10^3 M^{-1}). Compound **3** bound weakly to each studied protein. High resolution ESI qTOF mass spectra of albumin before and after binding of **1** revealed the high stoichiometry of binding. Although the binding of the compounds **1**–**3** to albumin and transferrin did not affect proteins' secondary structure much, their tertiary structures underwent some alterations, as deduced from the circular dichroism study. Changes in the stability of albumin, after binding to compounds **1**–**3** were examined by differential scanning calorimetry.

1. Introduction

A great number of human proteins, especially enzymes, contain metal ions at their active sites, and these metal ions play key catalytic and structural roles. Platinum-based drugs (cisplatin, carboplatin, and oxaliplatin) have been among the most effective chemotherapeutic agents in cancer treatment for years. However, their high toxicity and the incidence of spontaneous or acquired drug resistance limit their clinical use. To overcome these drawbacks, a huge number of coordination compounds of transition metals other than platinum has been thoroughly studied (Dyson and Sava, 2006; Jakupec et al., 2008; Motswainyana and Ajibade, 2015). Iron compounds with exciting potent anticancer activity, mediated by production of reactive oxygen species have been tested, but their toxicity remains a challenge (Wani et al., 2016). The development of copper-based compounds as potential drugs is hindered by their extremely poor aqueous solubility, making it difficult to evaluate them in preclinical models or patients (Wehbe et al., 2016). The unique properties of ruthenium-based drugs such as rich synthetic chemistry, a range of oxidation states (Ru^{II}, Ru^{III} and Ru^{IV}), slow ligand exchange rates (close to those in cellular processes), favourable water solubility and less toxicity than that of conventional platinum drugs justify the great expectations posed for ruthenium compounds (Ang and Dyson, 2006; Bergamo et al., 2012; Motswainyana and Ajibade, 2015). Furthermore, their octahedral geometry enables them to bind to nucleic acids by new and unique ways (Bergamo et al., 2012).

Two coordination compounds of ruthenium(III), KP1019, indazolium *trans*-[tetrachlorobis(1*H*-indazole) ruthenate(III)] and NAMI-A, imidazolium *trans*-[tetrachloro(1*H*-imidazole)-(*S*-dimethyl sulphoxide)ruthenate(III)] (Bergamo et al., 2012), have been extensively studied as potential anti-tumour drugs and both compounds proved beneficial in phase I clinical trials (Hartinger et al., 2008; Rademaker-Lakhai et al., 2004). Two organometallic Ru(II) arene compounds, having a "piano-stool" configuration, have been investigated preclinically, RAPTA-C, ([$Ru(\eta^6$-*p*-cymene)Cl_2(pta)]; pta = 1,3,5-triaza-7-phosphaadamantane (Weiss et al., 2014) and RAED-C, [$Ru(\eta^6$-*p*-cymene)Cl(en)] (Aird et al., 2002).

A typical functional ruthenium coordination compound is activated by aquation, when its weakly bound ligand(s) dissociate in solution, enabling the metal ion to bind coordinately to a biological target (Gianferrara et al., 2009). It is generally thought that the cytotoxic activity of Ru compounds originates from binding to DNA, i.e. DNA is their primary (the so-called classical) target. However, other ruthenium compounds may also bind to "non-classical" targets such as proteins and RNA (Ang and Dyson, 2006). Protein targets seem to play a more important role than DNA in the anti-metastatic activity of NAMI-A (Bergamo et al., 2012).

Whenever a ruthenium anticancer compound is synthesised, its cytotoxicity and DNA binding ability are checked (Ang and Dyson, 2006; Motswainyana and Ajibade, 2015). However, the interactions of ruthenium metallodrugs with specific cellular proteins relevant for carcinogenesis or metastasis, such as histones (Adhireksan et al., 2014; Wu et al., 2011), collagen (Sava et al., 2003), metallothionein-2 (Casini et al., 2009) or protein kinases (Meggers et al., 2007) are rarely reported. Therefore, the role of protein binding in the action of metallodrugs is a hot research topic.

A potential Ru-based metallotherapeutic would preferably be administered intravenously, which means that its interaction with serum proteins is of crucial importance (Jakupec et al., 2008). Investigation of its interaction with the most abundant serum proteins is an important step in the pharmacological characterisation of each novel candidate drug (Groessl et al., 2010). This includes an assessment of parameters such as the binding stoichiometry, binding constant and the number of specific binding sites. Apart from being drug delivery vehicles (Groessl et al., 2010), serum proteins may be involved in their inactivation (Bergamo et al., 2003). The most abundant ones are as follows: HSA, human serum albumin (c = 35–50 g L^{-1}), IgG, immunoglobulin G (c = 7–16 g L^{-1}) (Kratz and Beyer, 1998) and Tf, serum transferrin (c = 2.5–3.5 g L^{-1}) (Sun et al., 1999). HSA is a non-glycosylated globular protein of 585 amino acids (Dugaiczyk et al., 1982), accounting for about 60% of the total protein in blood serum (Kratz and Beyer, 1998). The binding ability of HSA for a metallodrug affects its distribution in the body, rate of metabolism and excretion (Kratz and Beyer, 1998). In plasma taken from a cancer patient treated with KP1019, most of the drug was bound to HSA (Sulyok et al., 2005). IgG is the second most abundant serum protein, but its interactions with ruthenium metallodrugs have rarely been studied (Martinčič et al., 2014). As the third most abundant, Tf is a glycosylated globular protein of 679 amino acids (Sun et al., 1999) that serves to transport iron in human blood (Vincent and Love, 2012). Approximately 30% of Tf molecules are iron-loaded (holoTf, holotransferrin), which leaves the unloaded protein (apoTf, apotransferrin) free for transport of other metals (Vincent and Love, 2012). The role of ruthenium-drug' binding to Tf has been a subject of much dispute (Bergamo and Sava, 2011). Despite the long-standing hypothesis that Tf serves as a mediator to deliver Ru anticancer compounds selectively into tumour cells via cell surface receptors for Tf, the number of which is increased in tumours (Ang and Dyson, 2006), only few reports have convincingly shown that this actually happens (Guo et al., 2013).

Besides organometallic coordination compounds of Ru(II) (Ang et al., 2011), ruthenium compounds with polypyridyl ligands have emerged as leading candidates for use as anticancer drugs (Ang and Dyson, 2006; Zhao et al., 2014). They most often contain the following: bpy, 1,10-phenanthroline (phen) or 2,2':6',2''-terpyridine (tpy). Considered as classical anticancer drugs, a large number of Ru(II) polypyridyl compounds have been screened for anticancer activity (Ang and Dyson, 2006), but their interactions with proteins have scarcely been studied.

We recently reported the synthesis of a series of ruthenium(II) terpyridine compounds, with the general formula *mer*-[$Ru(L_3)$(N-N)X][Y]$_n$, in which L_3 is either tpy or Cl-tpy; X is Cl or S-dimethyl sulphoxide (dmso-S); N-N is en, dach or bpy; Y is Cl, PF_6 or CF_3SO_3, and n = 1 or 2, depending on the nature of X (Rilak et al., 2014). Their high water-solubility (> 25 mg mL^{-1}) makes them very attractive as potential metallotherapeutics for intravenous application. Three

compounds from the series: [Ru(Cl-tpy)(en)Cl][Cl] (**1**), [Ru(Cl-tpy)(dach)Cl][Cl] (**2**) and [Ru(Cl-tpy)(bpy)Cl][Cl] (**3**) (Fig. 1) were chosen for investigation of their interactions with biologically important molecules. These compounds form monofunctional adducts with N7 of 9-methylguanine or guanosine-5'-monophosphate (Rilak et al., 2014). They bind strongly to calf thymus (CT) DNA (K_b = 10^4–10^5 M^{-1}), both covalently and non-covalently, intercalating between base pairs (Lazić et al., 2016), which means they can be referred to as classical compounds. In addition, coordinative bonding of compounds **1** and **2** to the imidazole ring of L-histidine (His) was also demonstrated (Lazić et al., 2016). Within this frame, we aimed to examine whether the chosen three Ru(II) terpyridine compounds bind to major metal-transporting proteins from human blood. In the study presented herein, we examined interactions of the three Ru(II) compounds: **1**, **2** and **3** (Fig. 1) with HSA and serum Tf. It is worth noting that most binding studies *in vitro* involved apoTf, whereas in the circulation, 30% of Tf is saturated with iron (Sun et al., 1999). To simulate the actual physiological situation, we used partially iron-saturated Tf (a mixture of apoTf and holoTf at 30% iron saturation), throughout our work. The interactions were studied using a battery of methods: inductively coupled plasma optical emission spectrometry (ICP OES), fluorescence quenching, circular dichroism (CD) and differential scanning calorimetry (DSC).

2. Experimental

2.1. Materials

The compounds [Ru(Cl-tpy)(en)Cl][Cl] (**1**), [Ru(Cl-tpy)(dach)Cl][Cl] (**2**) and [Ru(Cl-tpy)(bpy)Cl][Cl] (**3**) were synthesised as described recently. Microanalysis, ultraviolet-visible (UV-vis) spectroscopy and 1H nuclear magnetic resonance (NMR) spectroscopy were used to check their purity and the data and spectra agreed well with those already reported (Rilak et al., 2014). Molar masses of the ions of the compounds (without the outer chloride) are as follows: 464.33 (**1**), 518.42 (**2**) and 560.42 g mol^{-1} (**3**). Ultrapure water produced in a Milli-Q system (Millipore Inc.) was used throughout. Analytical or reagent grade chemicals were obtained from Sigma–Aldrich (St. Louis, MO, USA) or other commercial vendors. HSA (Catalog # A8763), bovine serum albumin (BSA, A7906) and partially iron saturated human serum Tf (T3309) were from Sigma Aldrich and used as received. Molar masses of the proteins employed in calculations were taken from the producers' information sheets: 66 437, 66 430 and 80 000 g mol^{-1} for HSA, BSA and Tf, respectively. Protein solutions were prepared in phosphate buffered saline (PBS, 20 mM phosphate, 100 mM NaCl, pH 7.40) and stored in the dark at 4 °C for no longer than 3 days. HSA concentration was checked by measuring the absorbance at 280 nm (A_{280}), using 37 219 M^{-1} cm^{-1} as the molar extinction coefficient ($\mathcal{E}_{280}$) (Ace et al., 1995). This is not applicable to Tf, as iron binding alters its $\mathcal{E}_{280}$ value in a nonlinear manner. The $\mathcal{E}_{280}$ of Tf falls somewhere between 83 800 and 93 000 M^{-1} cm^{-1}. Therefore, Tf was precisely weighed on an analytical balance, dissolved and the A_{280} of the solution checked (James and Mason, 2008).

2.2. Preparation of ruthenated protein adducts

To prepare protein adducts with the Ru(II) terpyridine compounds, a constant amount of HSA (2.5 mg) or Tf (2.5 mg) was incubated with increasing quantities of compounds **1**, **2** or **3** in a fixed total volume of 0.5 mL of 20 mM PBS pH 7.4, for 24 h at 37 °C in a thermal cycler with constant shaking. The final protein-to-ruthenium ratios were 1:1, 1:2, 1:5 and 1:10. Unbound compound was removed from the adducts by ultrafiltration, using centrifugal filter devices, with a molecular mass cut-off 10 kDa (Microcon, Millipore Inc.). To prevent possible aggregation of the proteins, the centrifugation speed never exceeded 7000*g*, whilst the temperature was kept constant at 10 °C. The adducts, recovered in the so-called retentates (0.1 mL), were then extensively washed with a working buffer (20 mM phosphate buffer, pH 7.4). Samples of HSA and Tf, incubated with the buffer alone and treated exactly as the other samples throughout, served as controls. The working buffer contained no additional salts or any other additives and was passed through a 0.45 µm filter (Sartorius) and degassed before each operation. The samples were finally adjusted to a volume of 2.0 mL with the working buffer and used as such in CD and DSC experiments. Samples for the ICP OES were similarly prepared, except that the incubation mixtures contained different amounts of HSA (2.0 mg) and Tf (1.66 mg), the retentates were not diluted at the end (0.1 mL) and the proteins were also incubated with the drug cisplatin.

2.3. General procedures

Stock solutions of Ru(II) terpyridine compounds **1**, **2** and **3** in ultrapure water were freshly prepared before each experiment. Their UV-vis spectra were checked each time, as were their mass spectra, which were obtained by matrix-assisted laser desorption and ionisation time of flight mass spectrometry (MALDI TOF MS). The UV-vis spectra were recorded at room temperature using the wavelength scanning mode (Fig. S1) on a Varian Cary 100 Bio double beam spectrophotometer (Palo Alto, CA, USA). The operating range was 200–900 nm and 1.0 cm pathlength quartz cuvettes (3.0 mL) were used. Mass spectra of the compounds were acquired in the positive reflectron mode

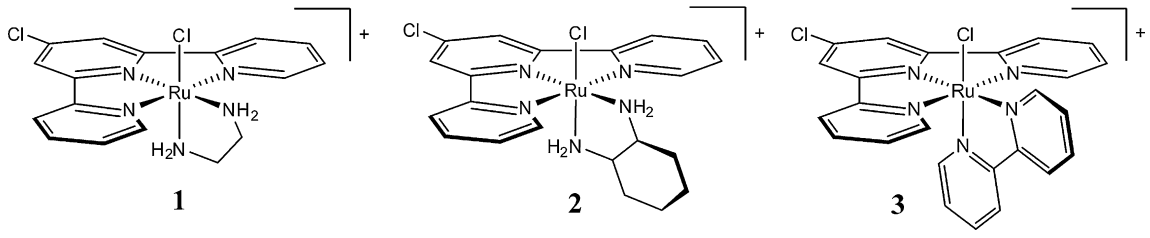

Figure 1 Chemical structures of the three Ru(II) terpyridine compounds under investigation: [Ru(Cl-tpy)(en)Cl]Cl **(1)**, Ru(Cl-tpy)(dach)Cl]Cl (**2**) and Ru(Cl-tpy)(bpy)Cl]Cl (**3**).

(Fig. S2) on a 4800 Plus MALDI TOF/TOF mass spectrometer (Applied Biosystems, Carlsbad, CA, USA) equipped with a 200 Hz, 355 nm Nd:YAG laser, as described elsewhere (Nišavić et al., 2016). ICP OES measurements were performed on a SPECTROFLAME-ICP Model P (Spectro Analytical Instruments, Kleve, Germany), operated at 27.12 MHz, 2.5 kW. ICP OES detected three spectral lines originating from ruthenium, the strongest occurring at 372.803 nm (Fig. S3), which was used both for calibration and for the measurements. The fluorescence measurements were run on a Varian Cary Eclipse spectrofluorometer operating at 25 °C, using a scan rate of 120 nm min^{-1}, an averaging time of 0.5 s, data collection every 1 nm and excitation and emission slit widths set to 5 nm and 10 nm, respectively. The fluorescence intensity was measured within the 310–450 nm range, upon excitation at 295 nm (excitation wavelength, λ_{exc}). The CD spectra were acquired at a constant temperature of 25 °C (Peltier temperature controller) over the wavelength 190–320 nm using a J-810 Jasco Spectropolarimeter, equipped with a xenon lamp and purged with nitrogen gas. The parameters were set as follows: resolution, 0.1 nm; scan speed, 50 nm min^{-1}; band width, 1.0 nm; response 1 s. The dynode voltage never exceeded 0.6 kV and the nitrogen flow was kept around 5 L min^{-1}. The instrument was calibrated for ellipticity units (in millidegrees) and wavelength (in nm) using (+)-10-camphorsulphonic acid at 290.5 nm. DSC analyses were done using Nano DSC (TA Instruments, New Castle, DE, USA). All the solutions were degassed prior to DSC runs. The adduct of BSA and compound **1** (BSA/**1** adduct) was prepared by incubating 15 μM protein solution with a 20-fold molar excess of **1**, in 50 mM ammonium bicarbonate buffer (pH 8.0) for 24 h, at 37 °C with constant shaking. The mass spectra of BSA and its adduct with compound **1** were recorded on a SYNAPT G2 system (Waters, Manchester, UK). The samples were introduced into the mass spectrometer via an Acquity ultra performance liquid chromatography (UPLC) column BEH130 C_{18} (100 μm × 100 mm; Waters, Milford) attached to a nanoAcquity UPLC system (flow rate 1 μl min^{-1}), coupled to the SYNAPT. The samples were diluted 1:10 in water and 5 μL was applied to a pre-column with a solution of acetonitrile/H_2O/HCOOH = 40:59.9:0.1 (*v*:*v*:*v*). The pre-column 2G-V/M 5 μm Symmetry C_{18} trap (180 μm × 20 mm), with a flow rate of 15 μl min^{-1} was used to desalt the samples prior to the MS analysis. The instrument conditions were as follows: capillary voltage 1.5 kV, sampling cone voltage 40 V, source temperature 80 °C, desolvation temperature 120 °C, acquisition window 500–4000 m/z in 1 s and source operating in the positive ionisation mode. Data were processed using the Mass Lynx 4.1 software.

2.4. ICP OES measurements

The samples of ruthenated and platinated protein adducts were subjected to overnight digestion in concentrated ultrapure nitric acid. The final volume was adjusted to 2.2 mL with 2% nitric acid. The samples were then analysed for their metal content. HSA and Tf samples incubated in the buffer without Ru compounds served as blanks. The Ru and Pt standards (NCS Analytica Instruments, 1000 μg mL^{-1}) were diluted with ultrapure water to make a 10 μg mL^{-1} stock solution, whilst the standards for calibration were freshly prepared by diluting the stock solution with 2% HNO_3. The concentrations used for calibration were as follows: 1, 2, 5 and 10 μg mL^{-1} (Fig. S4). The whole procedure was carried out twice; the samples were prepared in duplicates and two independent measurements were made for each sample.

2.5. Fluorescence quenching experiments

The protein/compound adducts were prepared by independently incubating a constant amount of protein with increasing amounts of compounds **1**, **2** or **3** in a fixed total volume of 2.0 mL 20 mM PBS pH 7.4 for 24 h, at 37 °C with constant shaking. The final molar ratios of protein-to-ruthenium were as follows: 1:0 (control), 1:1, 1:2, 1:3, 1:4, 1:5, 1:6, 1:7, 1:10, 1:12.5, 1:15 and 1:20. The concentrations of HSA and Tf were 2.5 μM and 2.6 μM, respectively. Emission spectra were recorded between 310 and 450 nm upon excitation at 295 nm immediately after the incubation using a quartz cuvette of 1.0 cm path length (Hellma Analytics). The emission spectra of solutions containing only the studied compounds (at the highest concentration) were also recorded under identical conditions. Appropriate blanks corresponding to the buffer were employed to correct the fluorescence background. Correction due to dilution effects was not necessary, because very small volumes (< 10 μL) of concentrated solutions of the compounds were added to the protein solutions. Absorbances of all the samples were measured between 250 and 450 nm, and the obtained values were used to correct the fluorescence data for the inner filter effect.

2.6. Circular dichroism studies

CD spectra of the ruthenated HSA and Tf samples were recorded both in the far UV (190–260 nm) and near UV (260–320 nm) region, using two types of Hellma quartz cuvettes: a demountable cuvette with a path length of 0.01 cm, for far UV, and one with a 1.0 cm-path length for near UV measurements. The samples were prepared in triplicates and four scans were accumulated for each sample. The CD spectrum of the buffer alone was subtracted from each spectrum. The concentrations of HSA and Tf were 18 μM and 15 μM, respectively.

2.7. Differential scanning calorimetry

DSC measurements were carried out over the temperature range 25–90 °C, following equilibration for 10 min at 25 °C. Temperature scan rate was 1 °C min^{-1}. Cell volume was 0.3 mL. The concentration of HSA was 18 μM.

3. Results and discussion

3.1. Binding stoichiometry for interactions between the Ru(II) terpyridine compounds and metal-transporting proteins

In our study, we have assessed the stoichiometry of binding between compounds **1**, **2** and **3** (Fig. 1) and HSA or Tf, using ICP OES. To prepare ruthenated or platinated protein adducts (HSA/metal or Tf/metal), the three compounds and cisplatin were individually incubated with HSA or partially iron-

Table 1 Metal (ruthenium or platinum) content of protein/metal adducts as determined by ICP OES. r_i indicates the initial protein-to-metal molar ratio in the incubation mixture; r_b is amount of Ru (or Pt) in the adducts, produced by incubation of human serum albumin (HSA) or partially-iron saturated human serum transferrin (Tf) with an excess of Ru(II) terpyridine compounds **1**, **2**, **3** or cisplatin for 24 h at 37 °C. The adducts were ultrafiltered through Microcon centrifugal filter devices (cut-off 10 kDa). Protein concentration was 11 μM. r_b is given as mol of Ru bound per mol of protein. Data shown are the mean ± SD of triplicate measurements. The reference drug cisplatin was used for comparison.

r_i	r_b			
	1	**2**	**3**	Cisplatin
(HSA/metal)				
1: 10 (3 h)	4.60 ± 0.12	5.30 ± 0.20	1.11 ± 0.22	1.28 ± 0.05
1: 10 (24 h)	6.92 ± 0.42	8.35 ± 0.25	1.51 ± 0.15	4.00 ± 0.01
(Tf/metal)				
1: 10 (24 h)	2.75 ± 0.30	3.36 ± 0.10	0.35 ± 0.01	2.00 ± 0.01

saturated human serum Tf for 24 h at 37 °C. The unbound ruthenium compound (or cisplatin) was removed from the reaction mixture by ultrafiltration (Guo et al., 2013). The ICP OES analysis of the protein adducts indicated that all three compounds bound to the metal-transporting proteins: HSA and Tf, although to different extents (Table 1).

Few general conclusions can be drawn from the data. The 3 h-incubation time was not long enough for complete binding of the studied compounds to HSA; compound **2** appeared to be the best protein binding partner (1 mol of HSA bound up to 8.35 mol of **2** for 24 h) and HSA displayed higher binding capacity for the three compounds than Tf (see Table 1).

The results for cisplatin binding to HSA and Tf agreed with those obtained by others (Guo et al., 2013; Timerbaev et al., 2004). It is worth noting that the method used to remove unbound drug can greatly affect the results. Low values were obtained by those who used size exclusion chromatography (Groessl et al., 2010), which may have been due to dissociation of weakly bound drug molecules from the protein.

The biological destiny of a metallodrug greatly depends on its distribution between free and bound forms, so the extent to which a drug binds to the major plasma proteins affects its biological actions in the body (Bergamo et al., 2003; Groessl et al., 2010). Although the stoichiometry of binding between Ru(III) drugs and human serum proteins is known from several reports, only a few such data exist for ruthenium(II) compounds. It was shown that Tf can be loaded with at least ten KP1019 equivalents (Pongratz et al., 2004). The content of ruthenium bound to Tf, found in our study after incubation with **1** or **2**, was roughly 3-fold greater than that obtained with Ru(II) compounds of the type [(η^6-arene)Ru(en)Cl][PF_6] (Guo et al., 2013).

Coordination of Ru(II) compounds **1** and **2** to His (Lazić et al., 2016), cysteine (Cys) and methionine (Met) (Rilak et al., 2015) has recently been demonstrated. The fact that HSA contains 16 His residues, one free Cys and six Met (Dugaiczyk et al., 1982), implies a great number of possible binding sites for these compounds. It is not surprising that HSA bound so many positively charged ions of **1** and **2**, because HSA has many negatively charged surface areas, the overall charge being −12.2 (Paul et al., 2015). On the other hand, the overall charge of Tf is low, just 0.4 (Paul et al., 2015), even though the protein contains 19 His residues, many of which are solvent-exposed (Macgillivray et al., 1982) and theoretically available for attachment of the studied compounds. Tf also contains nine Met residues (Macgillivray et al., 1982).

3.2. Binding affinities of serum metal-transporting proteins for the Ru(II) terpyridine compounds

Besides the stoichiometry, it is very important to determine the strength of interactions between Ru(II) terpyridine compounds **1**, **2** and **3** and major serum metal-transporting proteins. To this end, we measured the relative binding affinities of HSA and Tf for the above compounds (expressed as binding constants, K_b) using fluorescence quenching. λ_{exc} of 295 nm was chosen due to the exclusive excitation of tryptophan (Trp) residues in proteins (Lakowicz, 2006; Peters, 2008).

3.2.1. Interaction with HSA

Fluorescence quenching experiments were done by independently adding different amounts of compounds **1**, **2** or **3** (0–31.25 μM) to HSA solutions (2.5 μM) in 20 mM PBS pH 7.4. The mixtures were incubated for 24 h at 37 °C prior to the measurement.

Fig. 2 shows typical changes of fluorescence intensity of HSA in the presence of increasing amounts of **1** (HSA + **1**), **2** (HSA + **2**) or **3** (HSA + **3**) in the incubation mixtures. A substantial decrease in HSA fluorescence was observed with **1** and **2** in a concentration-dependent manner. Five molar excesses of compounds **1** and **2** quenched the fluorescence intensity of HSA to approximately 53% and 47% of the initial value, respectively.

The strong quenching of Trp-214 fluorescence points to conformational change of the hydrophobic cavity of subdomain IIA, where the Trp-214 residue is located (Peters, 2008). This change was, most probably, provoked by binding of compound **1** or **2** to HSA. Upon excitation at 295 nm, none of the three compounds showed any fluorescence emission in the range from 310 to 450 nm.

The characteristic HSA emission, centred at 347 nm, shifted slightly from 347 to 342 nm for HSA + **1** to 339 nm for HSA + **2**, respectively (Fig. 2). The observed blue shift is in accordance with the formation of ruthenated HSA adducts. The bonding altered microenvironment polarity in the vicinity of Trp-214 (Vivian and Callis, 2001). Compared to **1** and **2**, compound **3** lowered HSA fluorescence to a much smaller extent (a 10-fold molar excess of **3** quenched HSA fluorescence to just

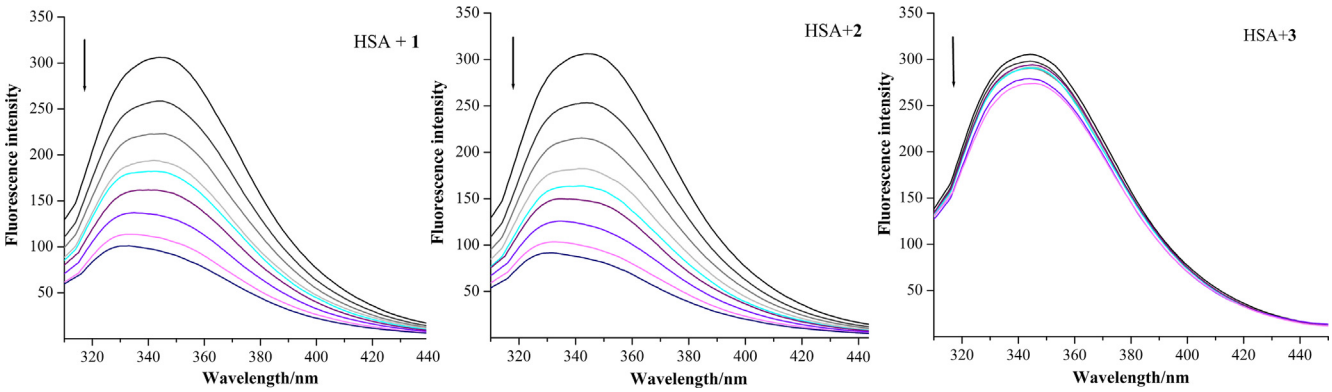

Figure 2 Fluorescence emission spectra of human serum albumin (HSA) and its adducts with Ru(II) terpyridine compounds **1** (HSA + **1**), **2** (HSA + **2**) and **3** (HSA + **3**). Samples were prepared by incubating increasing amounts of the compounds with a constant amount of protein in a buffer (20 mM phosphate, 100 mM NaCl pH 7.4), for 24 h at 37 °C. The final HSA concentration was 2.5 μM and that of the compounds ranged from 0 to 31.25 μM. λ_{exc} = 295 nm. The spectra were corrected for the inner filter effect.

90% of its initial value) without the blue shift (HSA + **3**). It is possible that the hydrophobic cavity in subdomain IIA of HSA was not sterically accessible to the rigid compound **3**.

The fluorescence intensities were corrected for the inner filter effect using Eq. (1), before being subjected to Stern-Volmer analysis (Eq. ((2)) (Lakowicz, 2006).

$$F_{corr} = F_{obs} \cdot 10^{\frac{A_{exc}+A_{em}}{2}} \quad (1)$$

$$\frac{F_0}{F} = 1 + K_{SV} \cdot [Q] = 1 + \tau_0 \cdot k_q \cdot [Q] \quad (2)$$

where F_{corr} and F_{obs} are the corrected and observed fluorescence intensities, respectively; A_{exc} and A_{em} are absorbances of incubation mixtures at 295 nm and 347 nm, respectively; F_0 and F are fluorescence intensities in the absence and presence of the quencher (studied ruthenium compounds), respectively; K_{sv} is the Stern-Volmer constant; k_q is the bimolecular quenching constant; τ_0 is the average lifetime of fluorophore

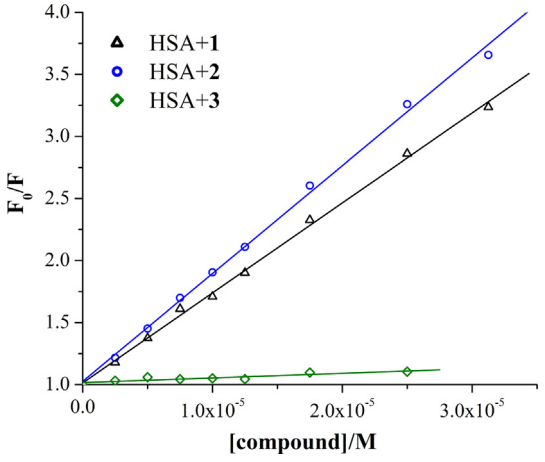

Figure 3 Stern-Volmer plots for quenching of human serum albumin (HSA, 2.5 μM) with increasing concentrations of the Ru (II) terpyridine compounds **1** (HSA + **1**), **2** (HSA + **2**) and **3** (HSA + **3**). The final concentration of the compounds ranged from 0 to 31.25 μM. λ_{exc} = 295 nm, λ_{em} = 347 nm. The solid line is a linear fit.

Table 2 Stern-Volmer data for the interaction of Ru(II) terpyridine compounds **1**, **2** and **3** with human serum albumin, as calculated from the fluorescence quenching experiments.

Compound	K_{SV} (10^4 M^{-1})	k_q (10^{12} M^{-1} s^{-1})	R
1	7.25 ± 0.13	12.08 ± 0.21	0.9989
2	8.70 ± 0.16	14.48 ± 0.27	0.9988
3	0.37 ± 0.73	0.62 ± 0.12	0.9009

in the absence of quencher; [Q] is the concentration of the quencher, i.e. [compound] (Lakowicz, 2006).

The plot of F_0/F versus [compound] was linear (Fig. 3) up to at least 12.5-fold excess of **1**, **2** or **3** over HSA. Linearity of the Stern-Volmer plots suggested the predominant involvement of one type of quenching (Lakowicz, 2006). The Stern-Volmer constants were calculated (Table 2). The K_{sv} values followed the pattern **2** > **1** ≫ **3**.

The bimolecular quenching constants, k_q were calculated from K_{SV} using Eq. (2) and assuming τ_0 = 6 ns for HSA (Lakowicz et al., 1980). 2×10^{10} M^{-1} s^{-1} is the maximal value of k_q resulting from collisional quenching of biopolymers (Lakowicz, 2006). The obtained k_q values were much higher than 2×10^{10} M^{-1} s^{-1} (Table 2), especially those for **1** and **2**. This finding strongly suggests predominance of static quenching of HSA fluorescence in the reaction with the studied compounds (i.e. the formation of ground state complexes).

The fluorescence data were then treated using the modified Stern-Volmer equation (Eq. (3)).

$$\log \frac{(F_0 - F)}{F} = n \cdot \log[Q] + \log K_b \quad (3)$$

The double logarithmic plots for all three studied compounds were linear (Fig. 4). K_b and the number of binding sites (n) for the interaction of HSA with **1**, **2** and **3** were calculated from the intercept and slope, respectively (Table 3).

K_b for compounds **1** and **2** lay within the range 10^4–10^5 M^{-1}, compound **2** being a slightly better binding partner for HSA than compound **1** (Table 3). The very low K_b for **3** was not unexpected, since it was not very effective at quenching fluorescence (HSA + **3**, Fig. 2). The relatively high K_b values for compounds **1** and **2** reflected moderate-to-strong

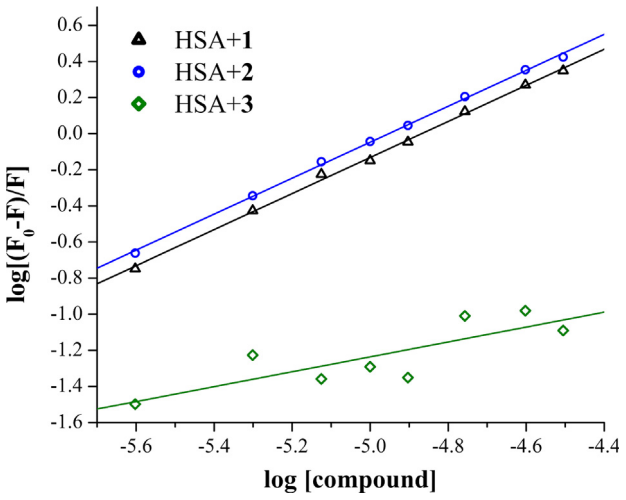

Figure 4 Double logarithmic plot for the quenching of human serum albumin fluorescence by Ru(II) terpyridine compounds **1** (HSA + **1**), **2** (HSA + **2**) and **3** (HSA + **3**). The solid line is a linear fit.

Table 3 Binding constants (K_b) and the number of binding sites (n) for interactions between human serum albumin and compounds **1**–**3**.

Compound	K_b (M^{-1})	n	R
1	$(7.19 \pm 0.0001) \times 10^4$	1.00 ± 0.02	0.9985
2	$(8.59 \pm 0.0001) \times 10^4$	1.00 ± 0.01	0.9994
3	6.72 ± 3.87	0.41 ± 0.12	0.8193

interactions between them and HSA, suggesting the formation of stable adducts. Therefore, upon intravenous administration, free concentrations of **1** and **2** in plasma would be low, as they would be mostly bound to HSA. In contrast to this, the low value of K_b for compound **3** implies weak binding to HSA and poor distribution in plasma.

Others reported similar K_b values ranging from 10^4 to 10^5 M^{-1} for binding of Ru((II) arene compounds to HSA (Beckford, 2010). Furthermore, Ru(II) polypyridyl compounds possessing bpy or phen ligands bound to HSA with K_b of approximately 10^5 M^{-1} (Sun et al., 2015). In accordance with published data we found only one specific binding site for compounds **1** and **2** on the HSA molecule (Sun et al., 2015).

3.2.2. Interaction with human serum transferrin

Fluorescence quenching was examined by independently adding different amounts of compounds **1**, **2** or **3** to solutions of Tf (2.6 μM) in 20 mM PBS pH 7.4. The mixtures were incubated for 24 h at 37 °C prior to the measurement. Intravenous administration of sodium salt of indazolium *trans*-[tetrachlorobis(1*H*-indazole) ruthenate(III)] (KP1339) resulted in a 20-fold excess of this compound over Tf in blood (Trondl et al., 2014). We used Tf-to-ruthenium ratios up to 1:20. As for quenching of HSA fluorescence (Fig. 2), Fig. S5 displays typical changes in Tf fluorescence with increasing amounts of compounds **1**, **2** and **3** in the incubation mixtures. At the Tf-to-ruthenium ratio of 1:10, fluorescence of the protein at the emission maximum (327 nm) dropped to approximately 81% and 77% of its initial value, for compounds **1** and **2**, respectively. Compound **2** showed slightly greater protein binding than **1,** whereas the binding of **3** was negligible as maximal quenching was 97% of the F_0 value. The fluorescence quenching curves (Fig. S5) stopped decreasing at Tf-to-ruthenium ratios greater than 1:12.5 (Tf + **2**), 1:10 (Tf + **1**) and 1:7 (Tf + **3**).

The fluorescence quenching data for the interaction between Tf and **1**, **2** or **3** were corrected for the inner filter effect using Eq. (1) and subjected to Stern-Volmer analysis using Eq. (2). The Stern-Volmer plots (Fig. S6) were linear, implying a single type of quenching (Mazuryk et al., 2012), so K_{sv} values were calculated from the slopes. Assuming 6 ns as the τ_0 value for Tf (Lakowicz et al., 1980; Mazuryk et al., 2012), the k_q values were also assessed (Table 4). The data were then analysed employing Eq. (3) and plotted in a double logarithmic plot (Fig. S7), which was then used to assess the binding parameters: apparent association constant (K_{app}) and n (Table 4).

The K_{sv} values we obtained with compounds **1** and **2** (Table 4) are concordant with that for NAMI-A binding to apo-Tf (Mazuryk et al., 2012). We found $k_q \sim 10^{12}$ M^{-1} s^{-1}, which implies some types of bonding between Tf and studied compounds **1** and **2**. Compound **3** bound weakly to Tf, probably due to steric hindrance around the ruthenium centre.

In contrast to HSA, which has Trp-214 as a single fluorophore (Peters, 2008), human Tf possesses eight Trp residues (Macgillivray et al., 1982). Since these residues are all more or less sensitive to changes in the local environment, the analysis of fluorescence quenching data is more difficult. A binding event that would quench the fluorescence of all Trp residues in Tf is not probable (Mazuryk et al., 2012). This is evident when one compares the quenching efficacy that compounds **1**, **2** and **3** exerted towards HSA with those towards Tf. Within this frame, the calculated binding constants do not represent true K_b, but rather K_{app}.

Published data on K_{app} for binding of ruthenium coordination compounds to Tf are scarce, if one excepts the few compounds in clinical testing. KP1019 bound to Tf with an K_{app} of 5.6–6.5 × 10^3 M^{-1} (Polec-Pawlak et al., 2006; Timerbaev et al., 2005).

To sum up the fluorescence quenching data, HSA appeared to be a much more active binder of the studied compounds than Tf and their relative binding affinity to both proteins followed the pattern: **2** > **1** ≫ **3**.

Table 4 Stern-Volmer quenching constants (K_{sv}), apparent association constants (K_{app}) and the number of binding sites (n) for the interacting system: partially iron-saturated human serum transferrin and Ru(II) terpyridine compounds **1**, **2** and **3**.

Compound	K_{sv} (10^3 M^{-1})	k_q (10^{12} M^{-1} s^{-1})	R	K_{app} (10^2 M^{-1})	n	R
1	7.51 ± 0.60	1.25 ± 0.09	0.9782	0.64 ± 0.02	0.54 ± 0.04	0.9793
2	11.42 ± 0.41	1.90 ± 0.07	0.9949	10.00 ± 0.01	0.77 ± 0.04	0.9916
3	2.39 ± 0.55	0.40 ± 0.09	0.8878	0.025 ± 0.03	0.36 ± 0.08	0.9298

3.3. Identification of ruthenium-serum albumin adducts by electrospray ionisation mass spectrometry

Mass spectrometry (MS) is becoming an important tool for studying interactions of coordination compounds of transition metals with model proteins (Hartinger et al., 2013). BSA is often employed to study interactions between serum albumin and (metallo)drugs, because it is structurally similar to HSA (Peters, 2008). With the aid of a high-resolution electrospray ionisation (ESI) qTOF MS, we detected a BSA adduct of the ion **1**, $[Ru(Cl\text{-}tpy)(en)Cl]^+$. The interactions that held the BSA/**1** adduct together were rather strong, since they persisted within the denaturing conditions in the UPLC column, through which the adduct passed on its way to the MS instrument. Using the MaxEnt algorithm (Waters), we deconvoluted the mass spectra of BSA and its ruthenated adduct onto a true mass scale (Fig. S8), and we obtained their accurate molecular masses. A peak at 66434.2109 Da dominated the spectrum of the free protein (intact BSA in Fig. S8). The molecular mass of BSA, calculated from its amino acid sequence, is 66430.3 Da. The deconvoluted mass spectrum of the adduct (BSA + **1** in Fig. S8) contained a major signal at 71954.98 Da. The signal was tentatively assigned to an adduct of composition: $\{BSA + 9\ [Ru(Cl\text{-}tpy)(en)]^{2+} + [Ru(Cl\text{-}tpy)(en)H_2O]^{2+} + 3\ [Ru(Cl\text{-}tpy)(H_2O)_2]^{2+} - 3H\}$ (Table 5).

Therefore, after dissociation of their inner chloride ions, nine moieties of the compound **1** would coordinately bind to a single BSA molecule; one Ru(II) moiety would first exchange inner Cl^- for a water molecule and then bind to BSA noncovalently; three ruthenium moieties would attach to BSA coordinately, after loosing their en ligands and inner Cl^- and adopting two water molecules. The dissociation of Cl^- from ruthenium compounds is considered necessary for their coordination to proteins (Casini et al., 2007, 2009; Groessl et al., 2010). Losing the en ligand from **1** was not unexpected, as some RAPTA compounds lost their pta ligand upon binding to proteins (Casini et al., 2007). Being smaller than $[Ru(Cl\text{-}tpy)(H_2O)_2]^{2+}$, $[Ru(Cl\text{-}tpy)(en)]^{2+}$ would be able to reach the less accessible electron donor groups in BSA. The $[Ru(Cl\text{-}tpy)(en)H_2O]^{2+}$ moiety most probably bound to BSA through electrostatic interactions with negatively charged amino acid residues on the protein (incubation mixture pH was 8.0, whilst pI of BSA is 4.7) (Peters, 2008).

Therefore, thirteen ruthenium moieties that originated from compound **1** bound to a single BSA molecule. BSA can bind up to 6 mol equivalents of **1** at a BSA-to-Ru ratio of 1:10 (Nišavić et al., 2016). This amount should be at least doubled at the BSA-to-Ru ratio of 1:20, which was examined in our MS experiment.

Table 5 Ruthenium functionalities assumed to bind to bovine serum albumin and their monoisotopic masses. The moieties that were detected in the MALDI TOF mass spectra of the compound **1** (Fig. S2) are marked with an asterisk.

The ruthenium functionality	Monoisotopic mass
$[Ru(Cl\text{-}tpy)(en)Cl]^+$	463.9983*
$[Ru(Cl\text{-}tpy)(en)]^{2+}$	429.0294
$[Ru(Cl\text{-}tpy)(en)(H_2O)]^{2+}$	447.0399
$[Ru(Cl\text{-}tpy)(H_2O)_2]^{2+}$	404.9818*

The high capacity of BSA for binding transition metals is logical as it possesses sixteen His residues (Hirayama et al., 1990), of which ten are reactive and solvent-exposed (Hnízda et al., 2008). BSA also contains one free Cys thiol group, four Met and an N-terminal amino group (Hirayama et al., 1990). Several reports have indicated His residues of serum albumins as sites of attachment of Ru(II) and Ru(III) moieties (Das et al., 2014; Hu et al., 2009; Webb and Walsby, 2015). We recently described coordination of **1** and **2** to several His residues in BSA (Nišavić et al., 2016).

In contrast to BSA, we still have no direct evidence for covalent binding of compounds **1** and **2** to serum Tf. In order to preserve the interactions of these compounds with Tf, which are obviously weaker than those with HSA, native MS would have to be performed. Not only is Tf a relatively large protein (76–81 kDa), but it carries two N-glycan chains with variable sugar content, which gives the protein a variable molecular mass (Sun et al., 1999). The small difference in mass between ruthenated and free Tf at a high charge state would make the native ESI mass spectra very difficult to resolve.

3.4. Conformational changes of serum albumin and transferrin upon binding of the Ru(II) terpyridine compounds

Any change in the native conformation of a protein may affect its function, and great alterations may be a biological signal for sending the protein down a degradation pathway. With this in mind, we examined the changes in secondary and tertiary structure of serum HSA and Tf following attachment of compounds **1**, **2** and **3**, using CD spectroscopy. The far UV CD spectra of HSA alone and its adducts with the studied compounds are shown in Fig. 5. To eliminate the potential influence of free (unbound) compounds on the CD spectra, the adducts were ultrafiltered before measurements. CD spectra of the filtrates (fraction < 10 kDa) showed no signals in the relevant wavelength range (190–320 nm).

A representative undistorted α helix displays two negative peaks in far UV CD spectra, with maxima at approximately 208 and 228 nm (Kelly and Price, 2000). We recorded an intense negative band with two peaks at 209 and 222 nm dominating the far UV CD spectra of free HSA (Fig. 5). Therefore, the spectra in Fig. 5 reflect the α helical secondary structure of HSA, which comprises mostly α helices (Carter and Ho, 1994). These spectra fit fairly well with the CD spectra of HSA reported by others (Liu et al., 2016; Luong et al., 2011; Peng et al., 2016; Samanta et al., 2014).

When comparing the spectrum of free HSA with those of its adducts with Ru(II) compounds **1**, **2** and **3** (Fig. 5), we observed no substantial differences, since all the spectra had a similar pattern. Furthermore, the intensity of the negative peaks at 209 and 222 nm showed little alteration upon the formation of adducts (see Table S1). The maximal difference between two measurements of a single sample was 2.6 mdeg, caused by the tricky packing of samples into a 0.01 cm demountable cell. Therefore, we came to the conclusion that, in general, the secondary structure of HSA did not alter after binding of studied compounds. Nevertheless, there were two minimal alterations of the original α helical structure of HSA: HSA/**1** adduct at a HSA-to-Ru ratio of 1:2 (slightly stabilising) and HSA/**3** adduct at a HSA-to-Ru ratio of 1:5 (slightly destabilising). Samples prepared at HSA-to-Ru ratios

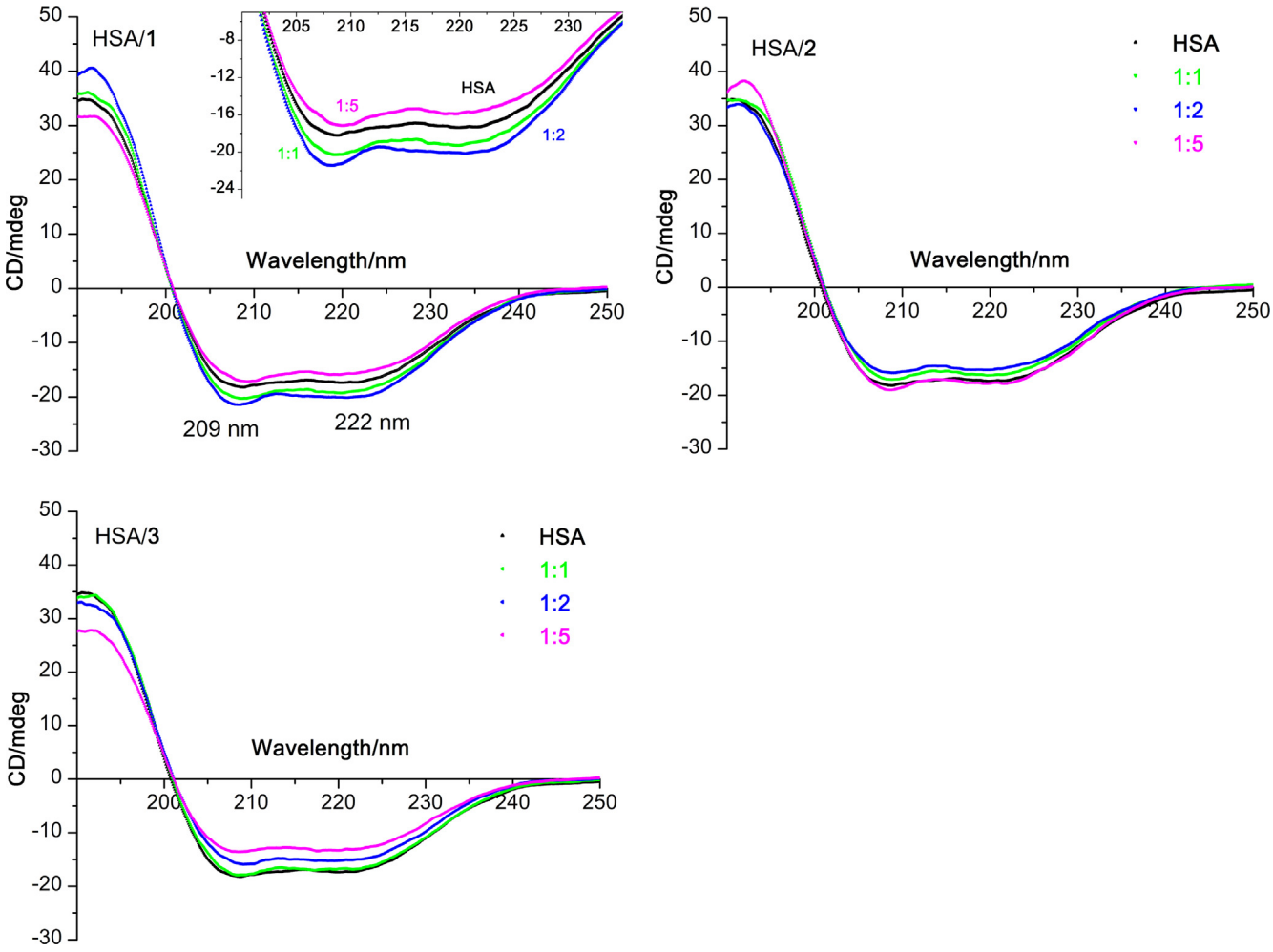

Figure 5 Far UV CD spectra of human serum albumin (HSA) and its adducts with Ru(II) terpyridine compounds **1** (HSA/**1**), **2** (HSA/**2**) and **3** (HSA/**3**). The inset shows the expansion of the region 200–235 nm. Samples were prepared by incubating increasing amounts of the compounds with a constant amount of protein for 24 h at 37 °C. Unbound compounds were removed from the HSA adducts by ultrafiltration. The buffer was 20 mM phosphate, pH 7.4. Protein concentration was 19 μM. The double minima at 209 and 222 nm originating from α helices are shown.

greater than 1:5 could not be measured, because their dynode voltage values exceeded 0.6, due to high absorption of the compounds in the far UV region (compare Fig. S1).

We recorded an intense negative band with two peaks at 209 and 222 nm dominating the far UV CD spectra of free Tf (Fig. 6). The spectra in Fig. 6 reflect the secondary structure of Tf, which comprises alternating α helices and β sheets (Sun et al., 1999). The far UV CD spectra of Tf (Fig. 6) are in good agreement with those previously published (Zhang et al., 2015). Binding of compounds **2** and **3** caused minimal (if any) changes in the secondary structure of Tf (see Table S1). However, there was a mild destabilisation of the α helicity with compound **1**, but only when applied at a Tf-to-Ru ratio of 1: 2. Binding of compound **3** to Tf caused no change of the spectra in Fig. 6 (Tf/**3**), which is in accordance with the very low value of K_{app} (Table 4) and the low stoichiometry of binding (Table 1). To sum up, the studied coordination compounds of Ru(II) bound to HSA and Tf generally without disturbing their secondary structures.

The CD spectrum of a protein in the near UV region (320–260 nm) reflects the microenvironment of aromatic side chains and disulphide bonds, being a fingerprint of the protein's tertiary structure. Aromatic amino acids give characteristic wavelength profiles: Trp, a peak in the region from 270 to 290 nm (Cooper, 2011) or 290–305 nm (Kelly and Price, 2000); tyrosine (Tyr), a peak between 270 and 280 nm; phenylalanine (Phe), a peak between 255 and 270 nm (Cooper, 2011; Kelly and Price, 2000). Fig. S9 shows a near UV CD spectrum of intact HSA in parallel with the spectra of HSA adducts with Ru(II) terpyridine compounds **1**, **2** or **3**. The spectra are consistent with the relevant ones obtained by others (Luong et al., 2011). Of all three tested compounds, compound **2** induced the smallest change in the tertiary structure of HSA (HSA/**2** in Fig. S9). The near UV CD spectrum of HSA differed from those for HSA/**1** and HSA/**3** adducts mainly in the 260–280 nm wavelength range, which is the fingerprint of Phe and Tyr residues. The negative signals became more negative, which indicated that HSA became more tightly folded

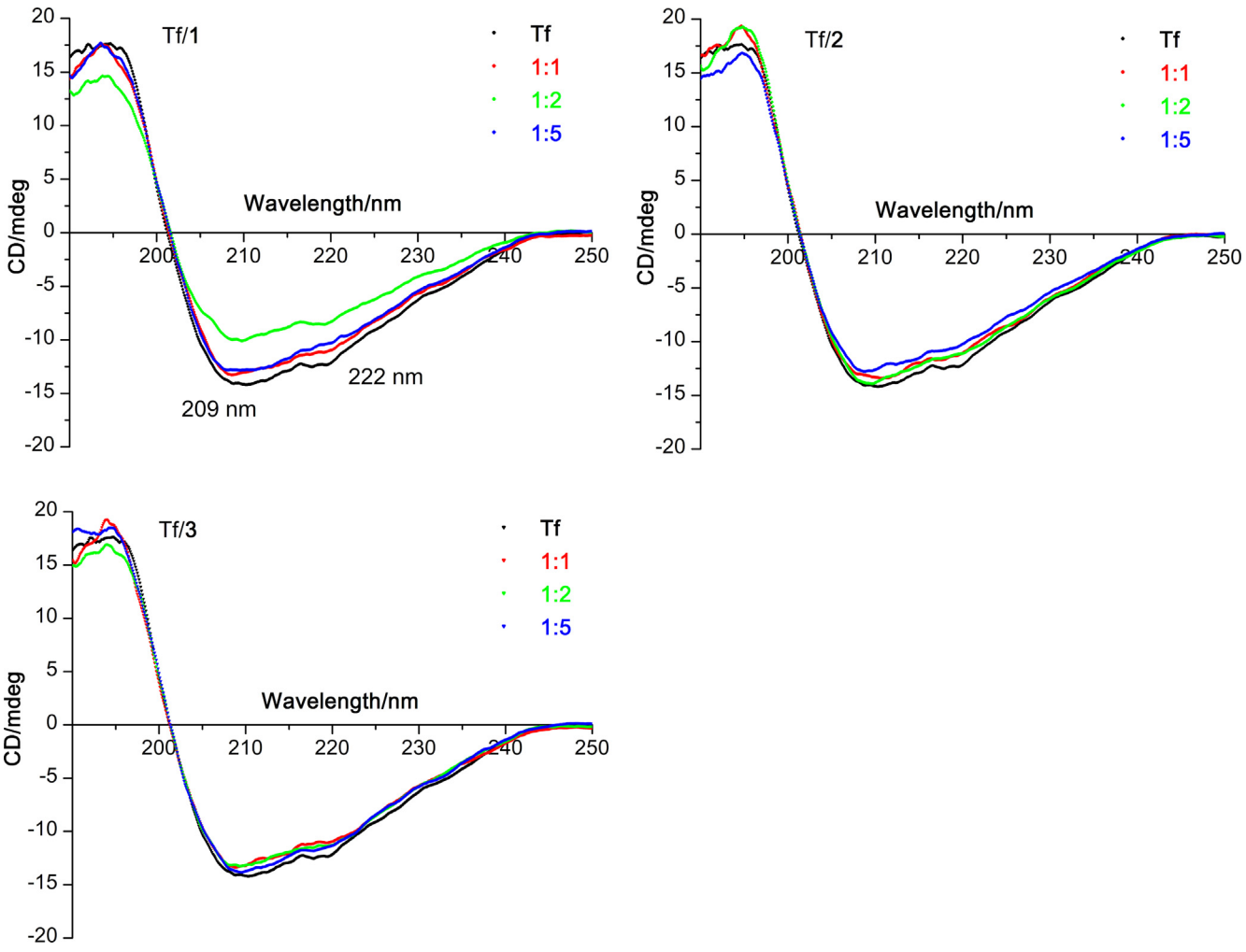

Figure 6 Far UV CD spectra of partially iron-saturated transferrin (Tf) and its adducts with Ru(II) terpyridine compounds **1** (Tf/**1**), **2** (Tf/**2**) and **3** (Tf/**3**). For the experimental conditions see Fig. 5. Protein concentration was 16 μM. The double minima at 209 and 222 nm originating from α helices are shown.

(Samanta et al., 2014) after binding **1** or **3**. However, drastic changes in the CD signals were absent, which meant that the tertiary structure of HSA suffered only slight modifications upon attachment of the compounds.

Fig. 7 displays near UV CD spectrum of intact Tf in parallel with spectra of Tf adducts with the Ru(II) compounds **1**, **2** or **3**. The spectrum of intact Tf was similar to those reported by others (Mehtab et al., 2013). A peak close to 290 nm originating from Trp is clearly visible. The spectra of Tf adducts (Tf/**1**, Tf/**2** and Tf/**3**) followed similar patterns (Fig. 7). The native conformation of Tf altered after binding the studied compounds, much more so in the region of Tyr signals than in the region dominated by Trp signals. Although the conformation of intact Tf altered with binding of compound **3** at a Tf-to-ruthenium ratio of 1:2, it did not change further at the Tf-to-ruthenium ratio of 1:10 (Fig. S10). This finding probably reflects a limited number of binding sites for compound **3** on Tf, which confirmed the results obtained by ICP OES (compare Table 1). Although ICP OES data suggested that Tf could accommodate more molecules of compounds **1** and **2**, near UV CD spectra of Tf/**1** and Tf/**2** adducts prepared at

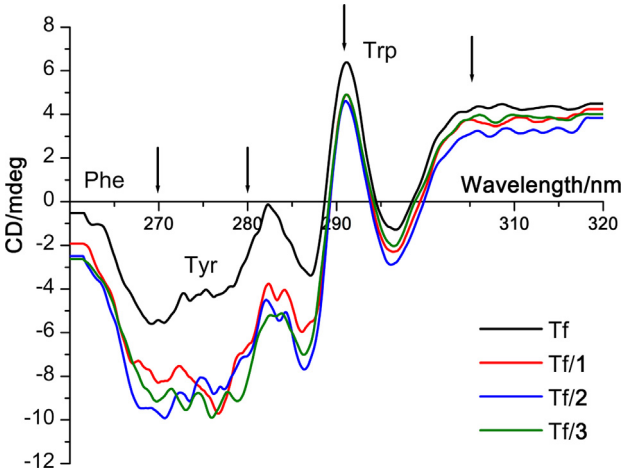

Figure 7 Near UV CD spectra of intact human serum transferrin (Tf) and its adducts with Ru(II) terpyridine compounds **1** (Tf/**1**), **2** (Tf/**2**) and **3** (Tf/**3**). A protein-to-ruthenium ratio of 1:2 was used in preparation of the adducts. Protein concentration was 16 μM. The arrows designate the wavelength ranges where signals from the aromatic amino acid residues were expected to appear.

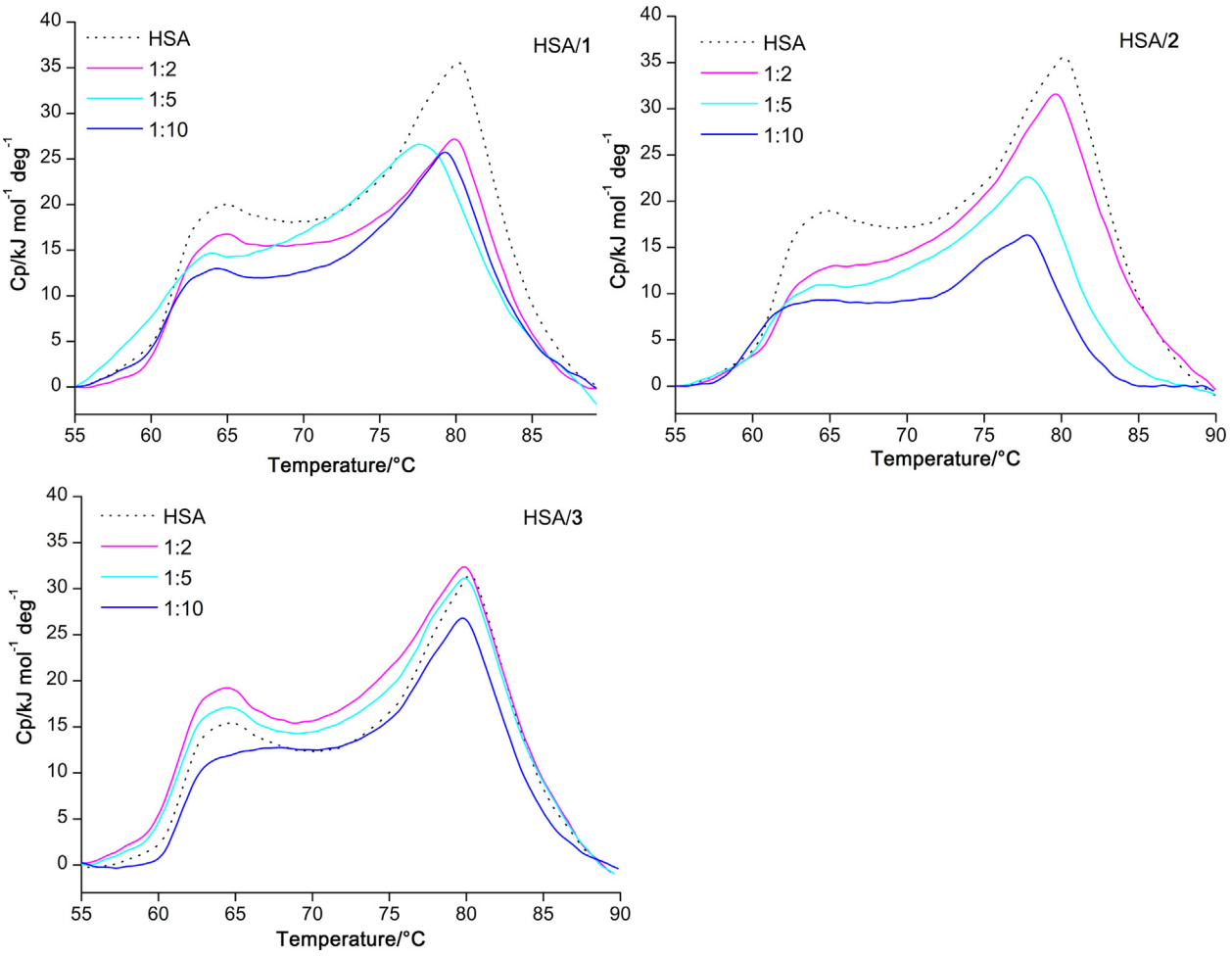

Figure 8 DSC thermograms of human serum albumin (HSA) and its adducts with Ru(II) terpyridine compounds **1** (HSA/**1**), **2** (HSA/**2**) and **3** (HSA/**3**), prepared at three different protein-to-ruthenium ratios, in 20 mM phosphate buffer pH 7.4. Protein concentration was 19 μM.

Tf-to-ruthenium ratios of 1:5 and 1:10 were not recorded owing to the high dynode voltages.

3.4.1. Conformational changes of HSA as seen through DSC

The change in thermostability of a protein in the presence of a drug is the most obvious manifestation of drug binding (Celej et al., 2006). We monitored changes in the thermostability of HSA in the absence and presence of increasing amounts of compounds **1**, **2** or **3** using DSC. The same samples that went through the CD measurements were afterwards subjected to DSC, which was set to run from 25 to 90 °C at the speed of 1 °C min^{-1}. The results are shown in the form of heat capacity at constant pressure (*Cp*) vs temperature curves (DSC thermograms) in Fig. 8.

Free HSA shows characteristic two-state thermally induced unfolding, with two endothermic peaks (Michnik et al., 2006). Two peaks were observed in bimodal thermograms in Fig. 8, which were then annotated as the first (T_m^1) and the second denaturation temperature (T_m^2). T_m^1 of free HSA in the buffer was approximately 65 °C and it did not show any significant change when the protein bound to the studied compounds (Table S2). T_m^2 of HSA in the buffer was found to be around 80 °C. Sometimes T_m^2 of HSA/**1** and HSA/**2** adducts were lower than T_m^2 of unbound HSA (Table S2), which was due to a shift in the equilibrium towards the denatured protein bound to the compounds. Compound **3** generally did not affect the thermal stability of HSA, mostly due to low reactivity with the protein. That compound **3** reacts poorly with HSA was also deduced from the fluorescence quenching (Fig. 2) and ICP OES (Table 1) measurements. Therefore, the results of the DSC study suggest that binding of the studied Ru(II) terpyridine compounds to HSA did not cause substantial conformational changes in the protein. This finding is consistent with that of the far UV CD study.

4. Conclusions

Three compounds were chosen from a series of coordination compounds of general formula $[Ru(Cl\text{-}tpy)(chel)Cl]^+$. Their interaction with two major metal-transporting proteins from serum, albumin and partially iron-saturated Tf, was addressed with an emphasis on the affinity and stoichiometry of the binding. Compared to Tf, HSA appears to be a more favourable binding partner for the studied ruthenium compounds. The affinity of the two proteins for **1**, **2** and **3** was evaluated using fluorescence quenching studies. Moderate-to-strong binding of compounds **1** and **2** to HSA was found, whereas their affinity for Tf was much lower. Compound **3** bound weakly to the proteins. The

compounds containing en and dach were more reactive with HSA and Tf than the compound with bpy, possibly due to easier release of chloride. The large capacity of serum albumin for binding **1** was detected using high resolution ESI qTOF mass spectrometry and highly purified BSA as a representative of serum albumins. The binding of the compounds to HSA and Tf did not affect secondary structures of the proteins much, whilst their tertiary structures showed some alterations. This finding is important, knowing that the native conformation of a transport protein should not be markedly altered upon binding a drug. Such as occurrence may prevent the protein from performing its normal actions (i.e. bind to cellular receptors and deliver the drug) or it may even be sent down a degradation pathway. Overall, our study implies that proteins are biological targets of the Ru(II) terpyridine compounds that contain bidentate aliphatic diamines such as en or dach. Investigations of this type are a key to understanding the transport and pharmacokinetics of potential anticancer drugs. The anti-metastatic properties of the ruthenium compounds, their interactions with intracellular proteins and their uptake by cancer cells are currently being examined and the findings will be reported elsewhere.

Acknowledgements

This study was supported by the Ministry of Education, Science and Technological Development of the Republic of Serbia: (grant No. 172011), Ministry of Science, Education and Sport of Croatia (grant No. 098-0982914-2918) and FP7-REGPOT-2012-2013-1, (Grant No. 316289 - InnoMol). Part of the work was supported by a STSM Grant from COST Action BM1403. None of the listed funding sources had any role in the study design, collection, analysis and interpretation of data: in the writing of the report or in the decision to submit the article for publication. The authors wish to thank Dr Mario Cindrić, Head of Centre for Proteomics and Mass Spectrometry, Division of Molecular Medicine, Ruđer Bošković Institute, Zagreb, Croatia, for performing the ESI qTOF MS measurements and Dr Marija Matković (Division of Organic Chemistry and Biochemistry, Ruđer Bošković Institute, Zagreb, Croatia), for her help with the CD measurements.

Appendix A. Supplementary material

Supplementary data associated with this article can be found, in the online version, at http://dx.doi.org/10.1016/j.arabjc.2016.07.021.

References

Ace, C.N., Vajdos, F., Fee, L., Grimsley, G., Gray, T., 1995. How to measure and predict the molar absorption coefficient of a protein. Protein Sci. 4, 2411–2423.

Adhireksan, Z., Davey, G.E., Campomanes, P., Groessl, M., Clavel, C.M., Yu, H., Nazarov, A.A., Yeo, C.H.F., Ang, W.H., Dröge, P., Rothlisberger, U., Dyson, P.J., Davey, C.A., 2014. Ligand substitutions between ruthenium-cymene compounds can control protein versus DNA targeting and anticancer activity. Nature Commun. 5, 3462.

Aird, R.E., Cummings, J., Ritchie, A.A., Muir, M., Morris, R.E., Chen, H., Sadler, P.J., Jodrell, D.I., 2002. *In vitro* and *in vivo* activity and cross resistance profiles of novel ruthenium (II) organometallic arene complexes in human ovarian cancer. Br. J. Cancer 86, 1652–1657.

Ang, W.H., Dyson, P.J., 2006. Classical and non-classical ruthenium-based anticancer drugs: towards targeted chemotherapy. Eur. J. Inorg. Chem. 2006, 4003–4018.

Ang, W.H., Casini, A., Sava, G., Dyson, P.J., 2011. Organometallic ruthenium-based antitumor compounds with novel modes of action. J. Organomet. Chem. 696, 989–998.

Beckford, F.A., 2010. Reaction of the anticancer organometallic ruthenium compound, [(*p*-cymene)Ru(ATSC)Cl] with human serum albumin. Int. J. Inorg. Chem. 2010, 975756.

Bergamo, A., Messori, L., Piccioli, F., Cocchietto, M., Sava, G., 2003. Biological role of adduct formation of the ruthenium(III) complex NAMI-A with serum albumin and serum transferrin. Invest. New Drugs 21, 401–411.

Bergamo, A., Sava, G., 2011. Ruthenium anticancer compounds: myths and realities of the emerging metal-based drugs. Dalton Trans. 40, 7817–7823.

Bergamo, A., Gaiddon, C., Schellens, J.H.M., Beijnen, J.H., Sava, G., 2012. Approaching tumour therapy beyond platinum drugs: status of the art and perspectives of ruthenium drug candidates. J. Inorg. Biochem. 106, 90–99.

Carter, D.C., Ho, J.X., 1994. Structure of serum albumin. Adv. Protein Chem. 45, 153–203.

Casini, A., Mastrobuoni, G., Ang, W.H., Gabbiani, C., Pieraccini, G., Moneti, G., Dyson, P.J., Messori, L., 2007. ESI-MS characterisation of protein adducts of anticancer ruthenium(II)-arene PTA (RAPTA) complexes. ChemMedChem 2, 631–635.

Casini, A., Karotki, A., Gabbiani, C., Rugi, F., Vašák, M., Messori, L., Dyson, P.J., 2009. Reactivity of an antimetastatic organometallic ruthenium compound with metallothionein-2: relevance to the mechanism of action. Metallomics 1, 434–441.

Celej, M.S., Dassie, S.A., González, M., Bianconi, M.L., Fidelio, G. D., 2006. Differential scanning calorimetry as a tool to estimate binding parameters in multiligand binding proteins. Anal. Biochem. 350, 277–284.

Cooper, A., 2011. Biophysical Chemistry. RSC Publishing, Cambridge.

Das, D., Dutta, A., Mondal, P., 2014. Interactions of the aquated forms of ruthenium(III) anticancer drugs with protein: a detailed molecular docking and QM/MM investigation. RSC Adv. 4, 60548–60556.

Dugaiczyk, A., Law, S.W., Dennison, O.E., 1982. Nucleotide sequence and the encoded amino acids of human serum albumin mRNA. Proc. Natl. Acad. Sci. USA 79, 71–75.

Dyson, P.J., Sava, G., 2006. Metal-based antitumour drugs in the post genomic era. Dalton Trans. 16, 1929–1933.

Gianferrara, T., Bratsos, I., Alessio, E., 2009. A categorization of metal anticancer compounds based on their mode of action. Dalton Trans. 37, 7588–7598.

Groessl, M., Terenghi, M., Casini, A., Elviri, L., Lobinski, R., Dyson, P.J., 2010. Reactivity of anticancer metallodrugs with serum proteins: new insights from size exclusion chromatography-ICP-MS and ESI-MS. J. Anal. At. Spectrom. 25, 305–313.

Guo, W., Zheng, W., Luo, Q., Li, X., Zhao, Y., Xiong, S., Wang, F., 2013. Transferrin serves as a mediator to deliver organometallic ruthenium(II) anticancer complexes into cells. Inorg. Chem. 52, 5328–5338.

Hartinger, C.G., Jakupec, M.A., Zorbas-Seifried, S., Groessl, M., Egger, A., Berger, W., Zorbas, H., Dyson, P.J., Keppler, B.K., 2008. KP1019, a new redox-active anticancer agent-preclinical development and results of a clinical phase I study in tumor patients. Chem. Biodivers. 5, 2140–2155.

Hartinger, C.G., Groessl, M., Meier, S.M., Casini, A., Dyson, P.J., 2013. Application of mass spectrometric techniques to delineate the modes-of-action of anticancer metallodrugs. Chem. Soc. Rev. 42, 6186–6199.

Hirayama, K., Akashi, S., Furuya, M., Fukuhara, K., 1990. Rapid confirmation and revision of the primary structure of bovine serum albumin by ESIMS and FRIT-FAB LC/MS. Biophys. Biochem. Res. Comm. 173, 639–646.

Hnízda, A., Šantrůček, J., Šanda, M., Strohalm, M., Kodíček, M., 2008. Reactivity of histidine and lysine side-chains with diethylpy-

rocarbonate – a method to identify surface exposed residues in proteins. J. Biochem. Biophys. Methods 70, 1091–1097.
Hu, W., Luo, Q., Ma, X., Wu, K., Liu, J., Chen, Y., Xiong, S., Wang, J., Sadler, P.J., Wang, F., 2009. Arene control over thiolate to sulfinate oxidation in albumin by organometallic ruthenium anticancer complexes. Chem. Eur. J. 15, 6586–6594.
Jakupec, M.A., Galanski, M., Arion, V.B., Hartinger, C.G., Keppler, B.K., 2008. Antitumour metal compounds: more than theme and variations. Dalton Trans. 2, 183–194.
James, N.G., Mason, A.B., 2008. Protocol to determine accurate absorption coefficients for iron-containing transferrins. Anal. Biochem. 378, 202–207.
Kelly, S.M., Price, N.C., 2000. The use of circular dichroism in the investigation of protein structure and function. Curr. Protein Pept. Sci. 1, 349–384.
Kratz, F., Beyer, U., 1998. Serum proteins as drug carriers of anticancer agents: a review. Drug Delivery 5, 281–299.
Lakowicz, J.R., Freshwater, G., Weber, G., 1980. Nanosecond segmental mobilities of tryptophan residues in proteins observed by lifetime-resolved fluorescence anisotropies. Biophys. J. 32, 591–601.
Lakowicz, J.R., 2006. Principles of fluorescence spectroscopy, third ed. Kluwer Academic Publisher, New York.
Lazić, D., Arsenijević, A., Bugarčić, Ž.D., Puchta, R., Rilak, A., 2016. DNA binding properties, histidine interaction and cytotoxicity studies of water soluble ruthenium(II) terpyridine complexes. Dalton Trans. 45, 4633–4646.
Liu, B.-M., Zhang, J., Hao, A.-J., Xu, L., Wang, D., Ji, H., Sun, S.-J., Chen, B.-Q., Liu, B., 2016. The increased binding affinity of curcumin with human serum albumin in the presence of rutin and baicalin: a potential for drug delivery system. Spectrochim. Acta A 155, 88–94.
Luong, T.Q., Verma, P.K., Mitra, R.K., Hamenith, M., 2011. Do hydration dynamics follow the structural perturbation during thermal denaturation of a protein: a tetrahertz absorption study. Biophys. J. 101, 925–933.
Macgillivray, R.T.A., Mendez, E., Sinha, S.K., Sutton, M.R., Lineback-Zins, J., Brew, K., 1982. The complete amino acid sequence of human serum transferrin. Proc. Natl. Acad. Sci. USA 79, 2504–2508.
Martinčič, A., Milačič, R., Vidmar, J., Turel, I., Keppler, B.K., Ščančar, J., 2014. New method for the speciation of ruthenium-based chemotherapeutics in human serum by conjoint liquid chromatography on affinity and anion-exchange monolithic disks. J. Chromatogr. A 1371, 168–176.
Mazuryk, O., Kurpiewska, K., Lewiński, K., Stochel, G., Brindell, M., 2012. Interaction of apo-transferrin with anticancer ruthenium complexes NAMI-A and its reduced form. J. Inorg. Biochem. 116, 11–18.
Meggers, E., Atilla-Gokcumen, G.E., Bregman, H., Maksimoska, J., Mulcahy, S.P., Pagano, N., Williams, D.S., 2007. Exploring chemical space with organometallics: ruthenium complexes as protein kinase inhibitors. Synlett 8, 1177–1189.
Mehtab, S., Gonçalves, G., Roy, S., Tomaz, A.I., Santos-Silva, T., Santos, M.F.A., Romão, M.J., Jakusch, T., Kiss, T., Pessoa, J.C., 2013. Interaction of vanadium(IV) with human serum apo-transferrin. J. Inorg. Biochem. 121, 187–195.
Michnik, A., Michalik, K., Kluczewska, A., Drzazga, Z., 2006. Comparative DSC study of human and bovine serum albumin. J. Therm. Anal. Calorim. 84, 113–117.
Motswainyana, W.M., Ajibade, P.A., 2015. Anticancer activities of mononuclear ruthenium(II) coordination complexes. Adv. Chem. 2015, 859730.
Nišavić, M., Masnikosa, R., Butorac, A., Perica, K., Rilak, A., Hozić, A., Petković, M., Koričanac, L., Cindrić, M., 2016. Elucidation of the binding sites of two novel Ru(II) complexes on bovine serum albumin. J. Inorg. Biochem. 159, 89–95.
Paul, L.E.H., Therrien, B., Furrer, J., 2015. Interactions of arene ruthenium metallaprisms with human proteins. Org. Biomol. Chem. 13, 946–953.
Peng, X., Wang, X., Qi, W., Su, R., He, Z., 2016. Affinity of rosmarinic acid to human serum albumin and its effect on protein conformation stability. Food Chem. 192, 178–187.
Peters, T., 2008. All About Albumin: Biochemistry, Genetics and Medical Applications, third ed. Academic Press, San Diego.
Polec-Pawlak, K., Abramski, J.K., Semenova, O., Hartinger, C.G., Timerbaev, A.R., Keppler, B.K., Jarosz, M., 2006. Platinum group metallodrug-protein binding studies by capillary electrophoresis – inductively coupled plasma-mass spectrometry: a further insight into the reactivity of a novel antitumor ruthenium(III) complex toward human serum proteins. Electrophoresis 27, 1128–1135.
Pongratz, M., Schluga, P., Jakupec, M.A., Arion, V.B., Hartinger, C. G., Allmaier, G., Keppler, B.K., 2004. Transferrin binding and transferrin-mediated cellular uptake of the ruthenium coordination compound KP1019, studied by means of AAS, ESI-MS and CD spectroscopy. J. Anal. At. Spectrom. 19, 46–51.
Rademaker-Lakhai, J.M., van den Bongard, D., Pluim, D., Beijnen, J. H., Schellens, J.H.M., 2004. A phase I and pharmacological study with imidazolium-*trans*-DMSO-imidazole-tetrachlororuthenate, a novel ruthenium anticancer agent. Clin. Can. Res. 10, 3717–3727.
Rilak, A., Bratsos, I., Zagrando, E., Kljun, J., Turel, I., Bugarčić, Ž. D., Alessio, E., 2014. New water-soluble ruthenium(II) terpyridine complexes for anticancer activity: synthesis, characterization, activation kinetics, and interaction with guanine derivatives. J. Inorg. Chem. 53, 6113–6126.
Rilak, A., Puchta, R., Bugarčić, Ž.D., 2015. Mechanism of the reactions of ruthenium(II) polypyridyl complexes with thiourea, sulfur-containing amino acids and nitrogen-containing heterocycles. Polyhedron 91, 73–83.
Samanta, N., Mahanta, D.D., Hazra, S., Kumar, G.S., Mitra, R.K., 2014. Short chain polyethylene glycols unusually assist thermal unfolding of human serum albumin. Biochimie 104, 81–89.
Sava, G., Zorzet, S., Turrin, C., Vita, F., Soranzo, M.R., Zabucchi, G., Cocchietto, M., Bergamo, A., DiGiovine, S., Pezzoni, G., Sartor, L., Garbisa, S., 2003. Dual action of NAMI-A inhibition of solid tumor metastasis: selective targeting of metastatic cells and binding to collagen. Clin. Cancer Res. 9, 1898–1905.
Sulyok, M., Hann, S., Hartinger, C.G., Keppler, B.K., Stingeder, G., Koellensperger, G., 2005. Two dimensional separation schemes for investigation of the interaction of an anticancer ruthenium(III) compound with plasma proteins. J. Anal. At. Spectrom. 20, 856–863.
Sun, H., Li, H., Sadler, P.J., 1999. Transferrin as a metal ion mediator. Chem. Rev. 99, 2817–2842.
Sun, J., Huang, Y., Zheng, C., Zhou, Y., Liu, Y., Liu, J., 2015. Ruthenium (II) complexes interact with serum albumin and induce apoptosis of tumour cells. Biol. Trace Elem. Res. 163, 266–274.
Timerbaev, A.R., Aleksenko, S.S., Polec-Pawlak, K., Ruzik, R., Semenova, O., Hartinger, C.G., Oszwaldowski, S., Galanski, M., Jarosz, M., Keppler, B.K., 2004. Platinum metallodrug-protein binding studies by capillary electrophoresis-inductively coupled plasma-mass spectrometry: characterization of interactions between Pt(II) complexes and human serum albumin. Electrophoresis 25, 1988–1995.
Timerbaev, A.R., Rudnev, A.V., Semenova, O., Hartinger, C.G., Keppler, B.K., 2005. Comparative binding of antitumor indazolium [*trans*-tetrachlorobis(1*H*-indazole)ruthenate(III)] to serum transport proteins assayed by capillary zone electrophoresis. Anal. Biochem. 341, 326–333.
Trondl, R., Heffeter, P., Kowol, C.R., Jakupec, M.A., Berger, W., Keppler, B.K., 2014. NKP-1339, the first ruthenium-based anticancer drug on the edge to clinical application. Chem. Sci. 5, 2925–2932.
Vincent, J.B., Love, S., 2012. The binding and transport of alternative metals by transferrin. Biochim. Biophys. Acta 1820, 362–378.

Vivian, J.T., Callis, P.R., 2001. Mechanisms of tryptophan fluorescence shifts in proteins. Biophys. J. 80, 2093–2109.

Wani, W.A., Baig, U., Shreaz, S., Shiekh, R.A., Iqbal, P.F., Jameel, E., Ahmad, A., Mohd-Setapar, S.H., Mushtaque, Md., Hun, L.T., 2016. Recent advances in iron complexes as potential anticancer agents. New J. Chem. 40, 1063–1090.

Webb, M.I., Walsby, C.J., 2015. Albumin binding and ligand-exchange processes of the Ru(III) anticancer agent NAMI-A and its bis-DMSO analogue determined by ENDOR spectroscopy. Dalton Trans. 44, 17482–17493.

Wehbe, M., Anantha, M., Backstrom, J., Leung, A., Chen, K., Malhotra, A., Edwards, K., Bally, M.B., 2016. Nanoscale reaction vessels designed for synthesis of copper-drug complexes suitable for preclinical development. PLoS ONE 11, e0153416.

Weiss, A., Berndsen, R.H., Dubois, M., Müller, C., Schibli, R., Griffioen, A.W., Dyson, P.J., Nowak-Sliwinska, P., 2014. *In vivo* anti-tumour activity of the organometallic ruthenium(II)-arene complex [Ru(η^6-*p*-cymene)Cl_2(pta)] (RAPTA-C) in human ovarian and colorectal carcinomas. Chem. Sci. 5, 4742–4748.

Wu, B., Ong, M.S., Groessl, M., Adhireksan, Z., Hartinger, C.G., Dyson, P.J., Davey, C.A., 2011. A ruthenium antimetastasis agent forms specific histone protein adducts in the nucleosome core. Chem. Eur. J. 17, 3562–3566.

Zhang, X.F., Chen, L., Yang, Q.F., Li, Q., Sun, X.R., Chen, H.B., Yang, G., Tang, Y.L., 2015. Study on the interaction of a cyanine dye with human serum transferrin. Luminescence 30, 1176–1183.

Zhao, Z., Luo, Z., Wu, Q., Zheng, W., Feng, Y., Chen, T., 2014. Mixed-ligand ruthenium polypyridyl complexes as apoptosis inducers in cancer cells, the cellular translocation and the important role of ROS-mediated signaling. Dalton Trans. 43, 17017–17028.